Electronic supplementary information

Layer-by-layer assembled magnetic molecularly imprinted nanoparticles for highly specific recovery of luteolin from honeysuckle leaves

Xuemeng Tian [a], Ruixia Gao [a,*], Yue Wang [a], Yulian He [b], Sameer Hussain [a], Jake Heinlein [b], Jiahao Tian [a], Lisa D. Pfefferle [b], Xiaoshuang Tang [c], Yuhai Tang [a]

[a] *School of Chemistry, Xi'an Jiaotong University, Xi'an, Shaanxi 710049, China*

[b] *Department of Chemical & Environmental Engineering, Yale University, New Haven, Connecticut 06520-8286, United States*

[c] *Department of Urology, The Second Affiliated Hospital of Xi'an Jiaotong University, Xi'an, Shaanxi 710061, China*

* Corresponding author：

E-mail: ruixiagao@xjtu.edu.cn (R. Gao).

Tel: +86 29 82655399; fax: +86 29 82655399.

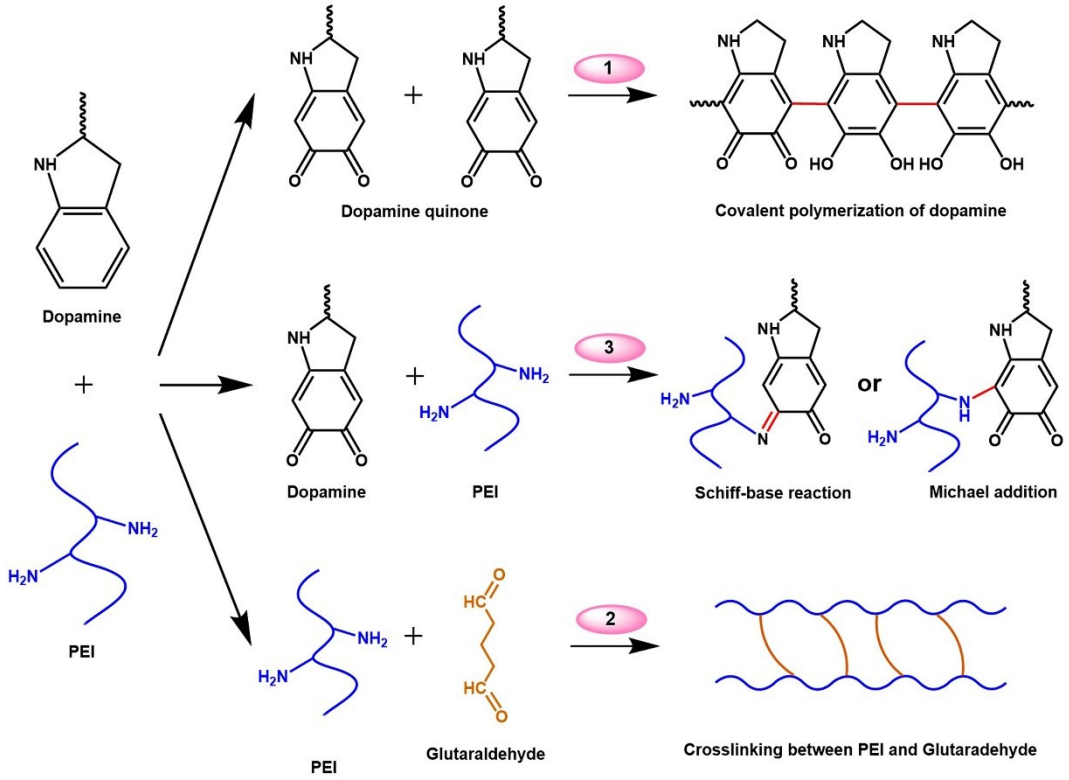

Scheme S1 Possible reactions for the co-deposition of dopamine/PEI [1].

The investigation of hydrogen bonding

The ^{1}H NMR and FTIR were used to investigate the hydrogen bonding between LTL and DA. ^{1}H NMR spectra of LTL, DA, and mixed LTL/DA in *d*-DMSO are presented in Fig. S1. The peak corresponding to N-H protons (a) in DA is located at δ 8.0[2,3]. It can be seen that the peak becomes broadened and a downfield shift to δ 8.8, attributing to the decrease in electron density around N-H protons resulting from the hydrogen-bonding complexation[4]. Similarly, the hydroxy protons (b) in LTL that appeared at δ 13.0 also becomes broadened, indicating hydrogen-bond formation between LTL and DA[5]. The results of ^{1}H NMR spectra provide complementary proof that the hydrogen bonding could be formed between the amino groups of DA in Fe_3O_4-LTL-MIPs and hydroxyl groups of LTL.

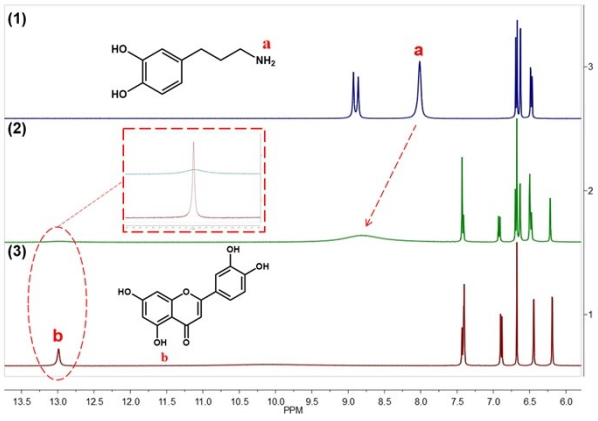

Fig. S1 ^{1}H NMR spectra of DA (1), mixed LTL/DA (2), and LTL (3) in *d*-DMSO.

Furthermore, the FTIR spectra of LTL (a), Fe_3O_4-LTL-MIPs (b), and Fe_3O_4-LTL-MIPs absorbed LTL (c) in $CHCl_3$ are given in Fig. S2. Peaks at 3463 and 3436 cm^{-1} are correspond to the stretching of O-H of LTL and N-H of the PDA layer in Fe_3O_4-LTL-MIPs, respectively. After absorption process, the broad peaks shift to lower frequency region i.e. 3415 cm^{-1}, signifying the weaken of bonds by additional hydrogen bonding[4]. The

appearance of new carbonyl peak in Fe_3O_4-LTL-MIPs absorbed LTL at lower frequency region 1608 cm^{-1} along with splitting further indicates that carbonyl takes part in hydrogen bonding interactions[6].

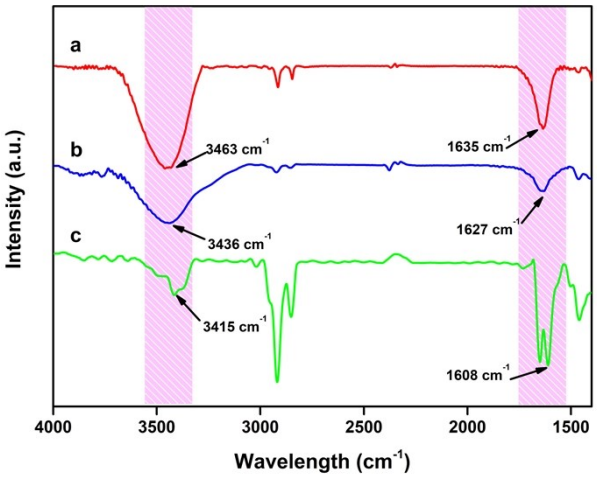

Fig. S2 FTIR spectra of LTL (a), Fe_3O_4-LTL-MIPs (b), and Fe_3O_4-LTL-MIPs absorbed LTL (c) in $CHCl_3$.

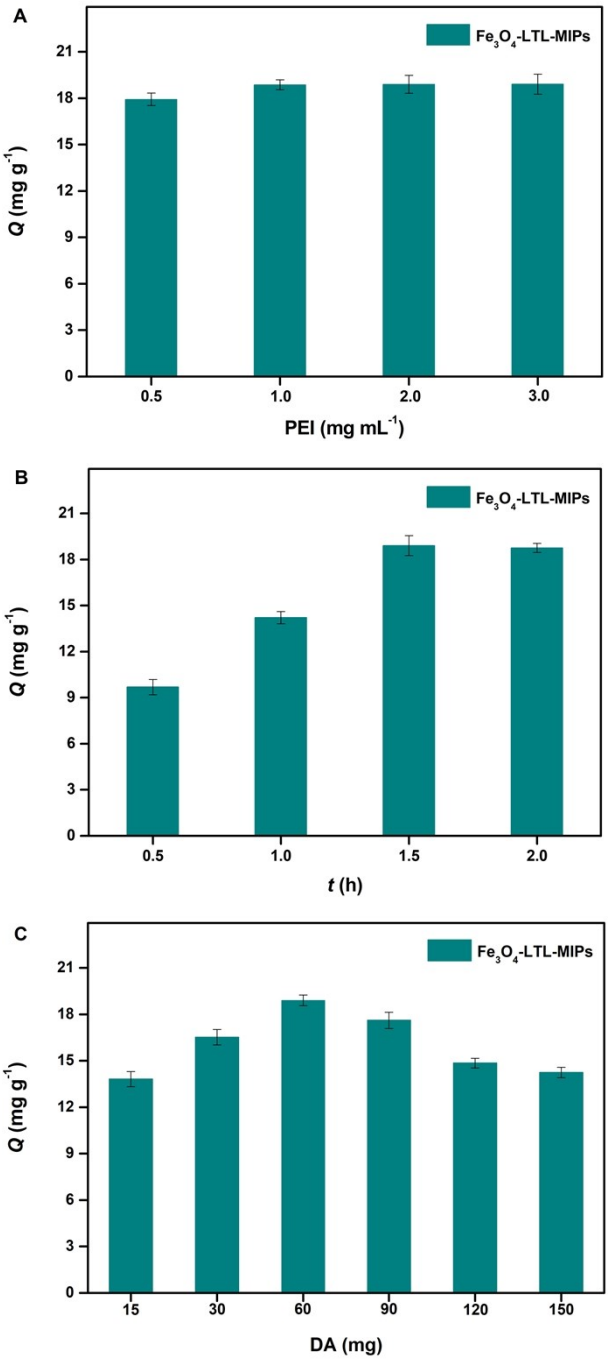

Fig. S3 Effect of the concentration of PEI (A), the immobilization time (B), and the amount of DA (C) on the absorption performance of Fe_3O_4-LTL-MIPs.

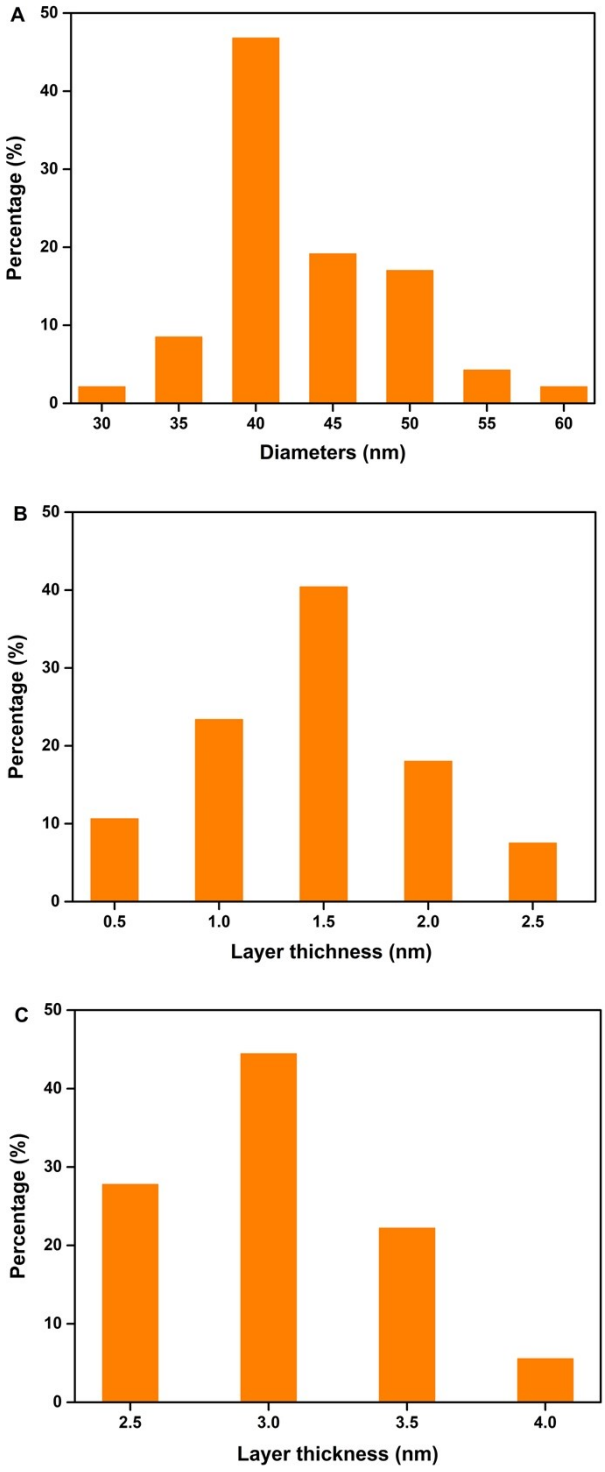

Fig. S4 The size distribution histogram of Fe_3O_4-NH_2 (A) and the layer thickness distribution of Fe_3O_4-PEI (B) and Fe_3O_4-LTL-MIPs (C).

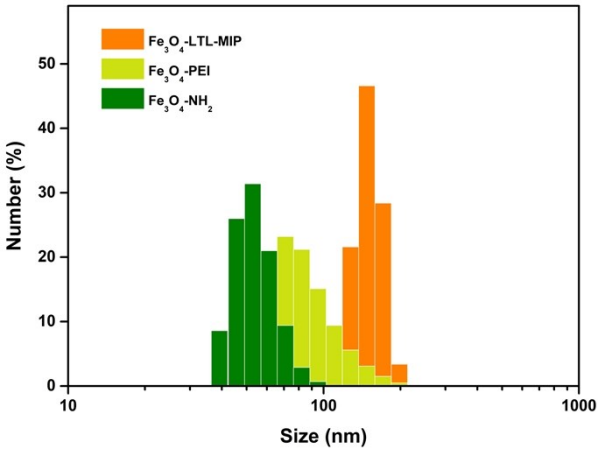

Fig. S5 DLS of Fe_3O_4-NH_2, Fe_3O_4-PEI, and Fe_3O_4-LTL-MIPs.

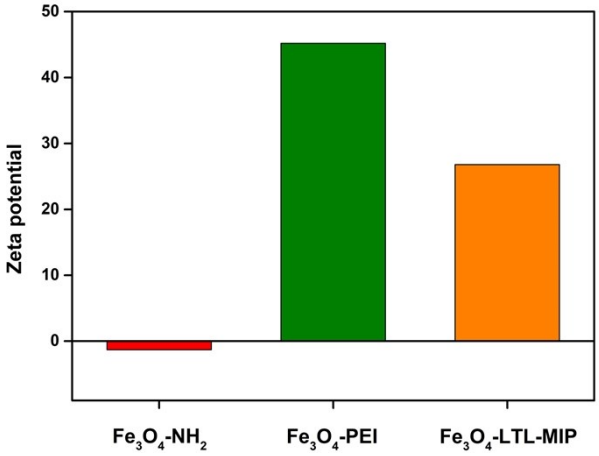

Fig. S6 The zeta potentials of Fe_3O_4-NH_2, Fe_3O_4-PEI, and Fe_3O_4-LTL-MIPs.

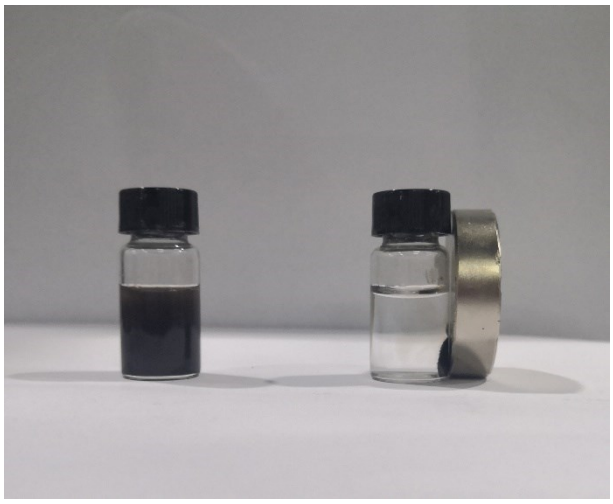

Fig. S7 The photographic image of the separation process of Fe_3O_4-LTL-MIPs with high concentration.

The XRD patterns of obtained nanomaterials

The XRD patterns of Fe_3O_4-NH_2, Fe_3O_4-PEI, and Fe_3O_4-LTL-MIPs in Fig. S8 show that six typical diffraction peaks (2ϑ = 30.15°, 35.46°, 43.09°, 53.61°, 57.20°, and 62.63°) are all observed. The peak positions at the corresponding 2ϑ values are indexed as (220), (311), (400), (422), (511), and (440), respectively. These 2ϑ values are in keeping with the database of magnetite in the JCPDS-International Center for Diffraction Data (JCPDS Card: 19-629) file.

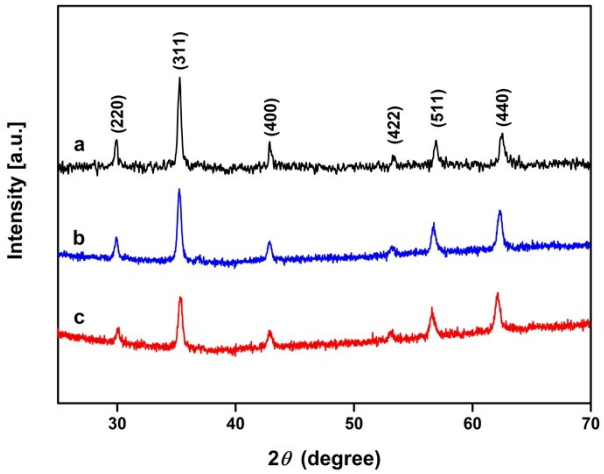

Fig. S8 XRD patterns of Fe_3O_4-NH_2 (a), Fe_3O_4-PEI (b), and Fe_3O_4-LTL-MIPs (c).

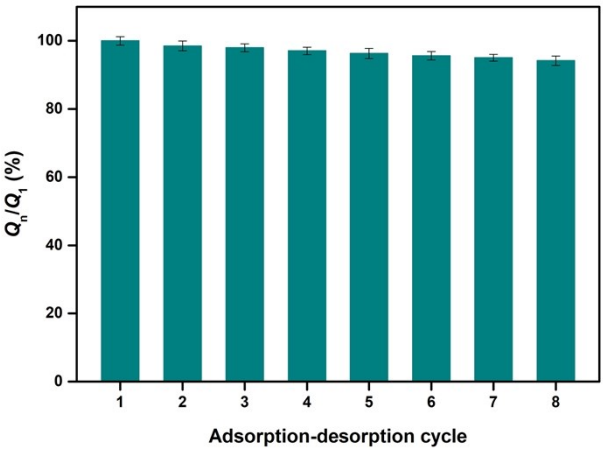

Fig. S9 Reusability of Fe_3O_4-LTL-MIPs.

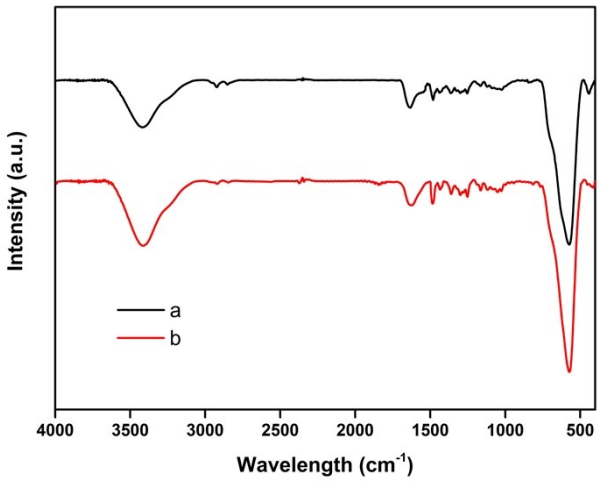

Fig. S10 FTIR spectra of Fe_3O_4-LTL-MIPs before (a) and after (b) the adsorption-desorption experiment.

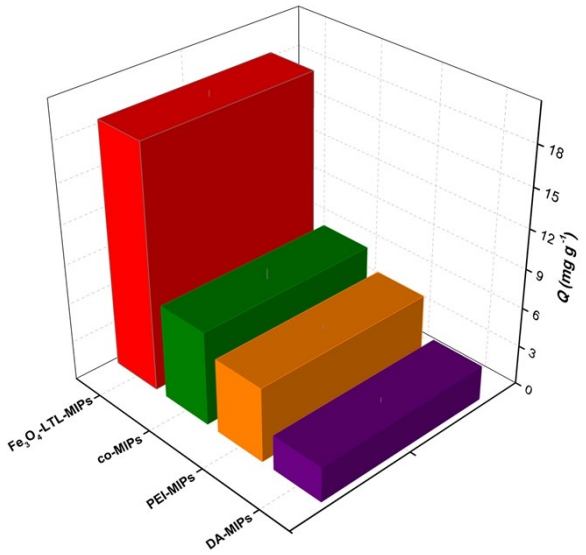

Fig. S11 The adsorption ability of Fe_3O_4-LTL-MIPs, co-MIPs, PEI-MIPs, and DA-MIPs in LTL solutions.

Table S1 Equations and parameters for the pseudo-first-order and pseudo-second-order kinetic models of Fe_3O_4-LTL-MIPs and Fe_3O_4-NIPs for LTL.

Model	Equations parameters	Fe_3O_4-LTL-MIPs	Fe_3O_4-NIPs
pseudo-first-order	Equation	$\ln (19.0 - Q_t) = \ln 19.0 - 1.688t$	$\ln (4.95 - Q_t) = \ln 4.95 - 1.582t$
	$Q_{e,f}$[a] (mg g^{-1})	19.0	4.95
	k_1 (min^{-1})	1.69	1.58
	R^2	0.960	0.927
pseudo-second-order	Equation	$t / Q_t = 0.0517t + 0.0077$	$t / Q_t = 0.2023t + 0.0201$
	$Q_{e,s}$[b] (mg g^{-1})	19.34	4.94
	k_2 (g mg^{-1} min^{-1})	0.35	2.04
	v_0 (mg g^{-1} min^{-1})	129.9	49.75
	R^2	0.999	0.996

[a] $Q_{e,f}$ (mg g^{-1}) is the calculated value of Q_e by pseudo-first-order equation.

[b] $Q_{e,s}$ (mg g^{-1}) is the calculated value of Q_e by pseudo-second-order equation.

Table S2 Equations and parameters for the *Langmuir* and *Freundlich* isotherm models of Fe_3O_4-LTL-MIPs and Fe_3O_4-NIPs for LTL.

Isotherm model	Equations and parameters	Fe_3O_4-LTL-MIPs	Fe_3O_4-NIPs
Langmuir isotherm	Equation	$C_e / Q_e = 0.0435C_e + 1.0291$	$C_e / Q_e = 0.1511C_e + 5.1271$
	K_L (mL mg^{-1})	42.27	29.46
	$Q_{m,L}$[a] (mg g^{-1})	22.99	6.62
	R^2	0.994	0.993
Freundlich isotherm	Equation	$\log Q = 0.3463 \log C_e + 0.5843$	$\log Q = 0.5202 \log C_e + 0.3329$
	K_F (mg g^{-1})	3.84	0.46
	m	0.35	0.52
	R^2	0.956	0.928

[a] $Q_{m,L}$ (mg g^{-1}) is the caculated value of Q_e by Langumuir isotherm equation.

Table S3 Selectivity adsorption parameters of Fe_3O_4-LTL-MIP and Fe_3O_4-NIP for LTL.

Analytes	Q_{MIP} (μmol g^{-1})	Q_{NIP} (μmol g^{-1})	*IF*	*SC*
LTL	66.03	16.74	3.94	-
QU	22.71	15.22	1.49	2.64
RT	7.90	3.99	1.98	1.99
CA	15.37	4.62	3.33	1.18
CH	8.04	2.23	3.61	1.09

Table S4 Reproducibility of Fe_3O_4-LTL-MIPs.

Nanomaterials	Batch	1	2	3	4	5	6	7	8	Average
Fe_3O_4-LTL-	Q (mg g^{-1})	18.64	19.29	18.48	18.93	19.04	18.87	18.45	18.80	18.81
MIPs	RSD (%)	5.2	3.3	4.7	4.0	3.7	4.1	3.8	4.3	1.5

References

1. Z. Dong, J. Zeng, H. Zhou, C. Lv, Y. Ma and J. Zeng, *J. Chem. Technol. Biotechnol.*, 2019, **94**, 942-954.

2. M. Vatankhah-Varnoosfaderani, S. Hashmi, A. GhavamiNejad and F. J. Stadler, *Polym. Chem.*, 2014, **5**, 512-523.

3. X. Ni, S. Rahman, S. Wang, C. Jin, X. Zeng, D. L. Hughes, C. Redshaw and T. Yamato, *Org. Biomol. Chem.*, 2012, **10**, 4618-4626.

4. T. Senthilkumar, F. Lv, H. Zhao, L. Liu and S. Wang, *ACS Appl. Bio Mater.*, 2019, **2**, 6012-6020.

5. S. Lee, J. Kim, H. Song, J. Seok, S. Hong and Y. Boo, *Antioxidants*, 2019, **8**, 87-98.

6. I. S. Ryu, X. Liu, Y. Jin, J. Sun and Y. J. Lee, *RSC Adv.*, 2018, **8**, 23481-23488.